IEEE Access
Multidisciplinary | Rapid Review | Open Access Journal

Received February 26, 2018, accepted March 28, 2018, date of publication April 24, 2018, date of current version May 9, 2018.

Digital Object Identifier 10.1109/ACCESS.2018.2827026

Coverage Analysis of Millimeter Wave Decode-and-Forward Networks With Best Relay Selection

KHAGENDRA BELBASE[1], (Student Member, IEEE), ZHANG ZHANG[2], (Member, IEEE), HAI JIANG[1], (Senior Member, IEEE), AND CHINTHA TELLAMBURA[1], (Fellow, IEEE)

[1]Department of Electrical and Computer Engineering, University of Alberta, Edmonton, AB T6G 1H9, Canada
[2]Department of Radio Access Network Research, Huawei Technologies Co., Ltd., Shanghai 201206, China

Corresponding author: Khagendra Belbase (belbase@ualberta.ca)

This work was supported in part by the Natural Sciences and Engineering Research Council of Canada and in part by the Huawei HIRP Project under Grant HO2016050002AY.

ABSTRACT In this paper, we investigate the coverage probability improvement of a millimeter wave network due to the deployment of spatially random decode-and-forward (DF) relays. The source and receiver are located at a fixed distance and all the relay nodes are distributed as a 2-D homogeneous Poisson point process (PPP). We first derive the spatial distribution of the set of decoding relays whose received signal-to-noise ratio (SNR) are above the minimum SNR threshold. This set is a 2-D inhomogeneous PPP. From this set, we select a relay that has minimum path loss to the receiver and derive the achievable coverage due to this selection. The analysis is developed using tools from stochastic geometry and is verified using Monte-Carlo simulation. The coverage probabilities of the direct link without relaying, a randomly chosen relay link, and the selected relay link are compared to show the significant performance gain when relay selection is used. We also analyze the effects of beam misalignment and different power allocations at the source and relay on coverage probability. In addition, rate coverage and spectral efficiency are compared for direct and selected relay links to show impressive performance gains with relaying.

INDEX TERMS 5G, decode-and-forward relay, millimeter wave communications, relay selection, stochastic geometry.

I. INTRODUCTION

The unprecedented growth in wireless data is expected to continue due to the emergence of data-intensive services and the massive and increasing number of connected wireless devices [1], [2]. Thus, fifth generation (5G) wireless networks are expected to provide high data rates (gigabits per second) along with low latency and high reliability [3], [4]. However, these targets will require a large bandwidth, which is a scarce resource because: (a) the sub-6 GHz bands are already allocated to existing wireless systems; and (b) the spectral efficiency of sub-6 GHz bands is already approaching the theoretical limits. Against this backdrop, millimeter wave (mmWave) frequency bands (20-100 GHz and beyond) offer huge bandwidth opportunities [2], [5], [6].

Unlike the sub-6 GHz bands, mmWave frequencies suffer very high propagation losses, possess directional channels, and exhibit sensitivity to blockages [7]. Blockages are common due to poor diffraction around the corners of the obstacles, causing very weak signal reception behind the obstacles [6]. Consequently, mmWave cellular networks have thus far remained elusive. Beamforming may compensate for high-path losses by using spatially compact large antenna arrays to focus the signal in desirable directions. Large arrays are possible because of the short mmWave wavelengths, resulting in significantly small antenna dimensions [2]. The feasibility of these bands has been established by mmWave propagation studies [6]–[8]. These studies also show that, unlike sub-6 GHz bands, substantially different path-loss exponents characterize line-of-sight (LOS) and non-line-of-sight (NLOS) regions. Consequently, mmWave links are susceptible to outage and poor coverage even at nearby NLOS receivers [8].

A. RELATED WORKS

Despite the propagation challenges and motivated by potential 5G applications, various researchers have investigated the performance of mmWave networks [9]–[14] using stochastic geometry techniques. For example, the work in [9] develops a general framework to analyze coverage and data rate. It considers blockages, directional antenna gains, mmWave channel models, random locations of base stations (BSs) and users, and their association probabilities to LOS or NLOS BSs. A tractable fixed ball LOS model which considers mmWave links for user access in lognormal shadowed channels is derived in [10]. Using empirical path loss models, this model derives both coverage and rate distribution. By exploiting the coverage analysis in [9], the work in [11] develops a comprehensive analysis of mmWave cellular networks. Further, the work in [12] analyzes heterogeneous downlink coverage with multiple tiers of mmWave cells, and also includes sub-6 GHz macro cells. In [13], signal-to-interference distribution is derived to study the rate performance of one-way and two-way ad-hoc networks by considering directional antennas, random blockages, and random channel access, where the authors show a significant contribution of NLOS links to mitigate outages.

1) SUB-6 GHz RELAY WORKS

Relay deployment improves coverage, throughput and reliability [15]. Performance analyses of relay networks have been extensive and we briefly mention a few herein. Based on analysis of outage probability and average channel capacity, it is demonstrated that maximum signal-to-noise ratio (SNR) relay selection provides a full diversity order [16]. Reference [17] provides a unified analysis of two-hop amplify-and-forward (AF) relaying, with an exact cumulative distribution function (CDF), a probability density function (PDF) and a moment generating function (MGF) of the received SNR. The work in [18] considers one source, one destination, and multiple relays. The relays whose end-to-end SNR are above a threshold are selected to help, to exploit the diversity. In [19], a cognitive multi-hop decode-and-forward (DF) relay network with channel estimation errors is analyzed. Reference [20] considers multiple source-destination pairs, and each pair is assigned a fixed relay. Joint optimal bandwidth and power allocation are developed, with a target at sum rate maximization.

2) MmWave RELAY WORKS

Relaying may provide seamless coverage to NLOS regions such as the areas blocked by buildings and may also extend indoor coverage to outdoors [8]. Reference [21] provides the first multi-hop medium access control (MAC) protocol for 60 GHz mmWave relaying by utilizing the diffracted signals to overcome outages when the direct transmitter-receiver link is blocked. Optimal placement of dual-hop relays to overcome blockages and rain attenuation is proposed in [22]. Highly dense mmWave AF relays have been investigated to improve coverage [23]. The coverage probability is derived by considering spatially random relays, effect of blockage, and log-normal shadowing. Coverage of device-to-device mmWave relaying is analyzed in [24]. Two-way relay selection also provides substantial coverage improvements [25].

3) STOCHASTIC GEOMETRY BASED ANALYSIS OF RELAYS IN mmWave AND SUB-6 GHz BANDS

Existing research has focused on fixed network topologies, where the locations of users and relay nodes are fixed. However, deployment constraints and/or mobility occur in practice. Therefore, more realistically, it is assumed that the locations of the relay nodes follow a homogeneous Poisson point process (PPP). The PPP model is widely established in the wireless literature because of its analytical tractability [26].

For sub-6 GHz bands, relaying has been widely analyzed by modeling the locations of nodes as PPPs [27]–[32]. For instance, in [27], using tools from stochastic geometry, outage performance is analyzed for a DF relay network. This work has been extended to DF cognitive relay networks in [29]. In [30], coverage probability is analyzed for AF relays, where the locations of the relays form a homogeneous PPP. The achievable transmission capacity of relay-assisted device-to-device links has been analyzed in [31]. Simulation results for DF relaying in a cellular network are presented in [32], where the base stations, relays, and user nodes are distributed as PPPs. For mmWave bands, on the other hand, relaying has also been studied using stochastic geometry, albeit not so widely. For example, AF relays for one-way [23], [24] and two-way [25] relaying show significant improvement in coverage probability and spectral efficiency. However, the effect of small-scale fading is not considered in the analysis [23]–[25].

B. PROBLEM STATEMENT AND CONTRIBUTIONS

To the best of our knowledge, a comprehensive analysis of mmWave DF networks with best relay selection and taking into consideration the spatial randomness of relay nodes and small-scale fading has been lacking. Specifically, we are interested in the following questions. What is the impact of small-scale fading? What role does the spatial randomness of relay nodes play? What are the coverage and rate improvements possible with relay selection? What is the impact of beam-alignment errors? We will use both analysis and computational results to explore these questions.

The major contributions of this paper are as follows:

- To model mmWave small-scale fading, we consider Nakagami-m fading with different m values to represent LOS and NLOS cases [9]. Blockages from obstacles such as buildings in urban areas are also incorporated. We adopt the blockage model derived in [33], which uses random shape theory and randomly drawn blockage parameters. We model the locations of the mmWave DF relays as a homogeneous PPP in the $\mathbb{R}^2$ plane with the constant spatial density of $\lambda > 0$ nodes per unit area.

- To analyze the best relay selection, we first derive the spatial distribution of the decoding set of relays that meet the decoding SNR threshold. The locations of the relays in the decoding set form an inhomogeneous PPP whose spatial density $\hat{\lambda}(x)$ is non-uniform over $x \in \mathbb{R}^2$. This set is then partitioned into LOS and NLOS subsets and the distributions of the distance of the nearest relay in these subsets are derived. Using these distributions, we derive the association probabilities of the receiver to the LOS and NLOS sets.
- To quantify the performance of best relay selection, we derive coverage probability and show its significant improvement when compared to no-relaying case (e.g. with only direct link). We also derive coverage with non-selection, i.e., for a randomly-picked relay. Again, relay selection significantly outperforms the non-selection.
- Finally, to study the impact of various deployment constraints, we analyze the impact of beam alignment errors and the effect of power allocation at source and relay. We also provide the rate coverage probability, and the spectral efficiency to demonstrate the improved performance due to relaying.

We validate our theoretical derivations by comparing them with extensive Monte Carlo simulations.

We further emphasize that previous works, including [9]–[14], have not considered relay deployments. Other works on mmWave relaying [23]–[25] do not consider the effect of small-scale (multi-path) fading as they only include distance-dependent path loss or lognormal shadowing. They also do not consider DF relays. Note that multi-path components are not insignificant in NLOS scenarios [13], [34]. Therefore, different m factors for LOS and NLOS cases will paint a more realistic picture [9].

The rest of the paper is organized as follows. Section II presents the system model. Section III provides the performance analysis of the system and contains the main results of this paper. Section IV investigates the effect of beam alignment errors, different power allocation at the source and the relay, rate coverage, and spectral efficiency. Section V discusses the analytical and simulation results and finally section VI summarizes our work and provides the conclusion.

II. SYSTEM MODEL

In this section, we introduce our system model to evaluate the performance of the mmWave DF relay network.

A. NETWORK MODELING

We consider a mmWave wireless network with a source (S), a receiver (D) and a set of relays which are distributed in $\mathbb{R}^2$-plane according to a homogeneous PPP of density λ (Fig. 1). The fixed distance between S and D is denoted by W. S can communicate with D either directly or via a relay selected from the available set of relays. We denote a typical relay by R. S transmits with power P_S, and for simplicity, we assume all potential relay nodes have equal transmit power of P_R. The extension to unequal transmit powers of relays is straightforward and omitted. Without loss of generality, the receiver (D) is assumed to be located at the origin for the tractability of our analysis. In fact, any other location for the receiver provides the same performance in a homogeneous PPP due to Slivnyak theorem [35].

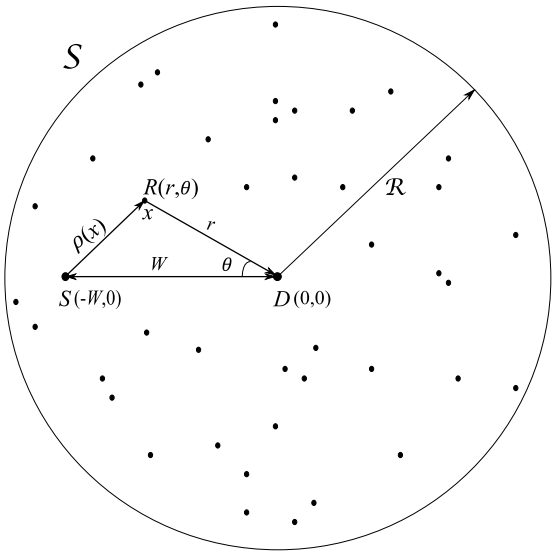

FIGURE 1. Geometrical locations of S, D and a typical relay (R).

The PPP is denoted by $\Phi = \{x_1, x_2, x_3, \ldots\}$, where $x_j \in \mathbb{R}^2$ is the location of the j-th relay, $j \in \{1, 2, \ldots, N\}$, and N is a Poisson random variable with mean $\lambda\pi\mathcal{R}^2$. Without loss of accuracy, we only consider the relay nodes inside the circular disc $\mathcal{S}$ of radius $\mathcal{R}$. The nodes outside $\mathcal{S}$ are ignored because of very high path loss and increased blockage probability associated with large distances. Therefore, $\mathcal{S}$ is essentially equivalent to entire $\mathbb{R}^2$ [25]. For notational convenience, x rather than x_j denotes the location of a typical relay node (R), and x is interchangeably used as a polar coordinate (r, θ).

B. BLOCKAGE MODELING

Blockage occurs when the transmitted signal cannot penetrate buildings, vehicles or other objects in urban areas, causing the transmitter-receiver link to be NLOS [36]. It has been shown that mmWave LOS and NLOS conditions have markedly different path loss exponents [36]. To model urban situations, the work in [33] develops a PPP based random blockage model. According to this model, the link of distance d can become LOS with probability $e^{-\beta d}$ where β is the blockage parameter. In the fixed LOS ball model [9], the irregular geometry of the LOS region is replaced with a circle of equivalent area whose radius determines the LOS probability. This model is also used in [10] to evaluate the self-backhauled mmWave based cellular network and has the main advantage of tractability of analysis, along with reasonable accuracy [37], [38]. In [12], [37], and [38], the fixed-ball LOS model is further extended to include general piecewise and multi-ball LOS probability functions to improve the

accuracy of the analysis. However, these approximations are difficult to use in the considered dual-hop network because each relay could fall under different LOS balls from S and D. Therefore, following [33], we assume that a link of length d has the LOS probability expressed as $p_L(d) = e^{-\beta d}$, and the NLOS probability expressed as $1 - p_L(d)$. The constant β is the blockage density parameter, which is obtained from the size and density of blocking obstacles.

C. DIRECTIONAL BEAMFORMING MODELING

Since high gain directional beams are needed to compensate for very high mmWave path loss [4], including directivity in the analysis is critical. Similar to [10], we approximate the directional gain using a simple sectored antenna model, in which the directional gain denoted as $G(\theta)$ takes value $G_{\max}$ if the azimuth angle θ is within the half power beamwidth (ϕ) and takes value $G_{\min}$ otherwise, mathematically shown as:

$$G(\theta) = \begin{cases} G_{\max} & \text{if } |\theta| \leq \frac{\phi}{2} \\ G_{\min} & \text{otherwise.} \end{cases}$$

The typical values of $G_{\max} = 18$ dBi, and $G_{\min} = -10$ dBi are considered in this study. Our subsequent analysis in Section III assumes perfect beam alignment for each link, and thus, the effective antenna gain is given as $G_{\text{eq}} = G_{\max}^2$. The effect of beam alignment errors is discussed in Section IV-A.

D. SMALL-SCALE FADING

The Rayleigh fading model is ubiquitous for sub-6 GHz bands, but is inaccurate for mmWave bands, especially with directional beamforming [6]. Therefore, the work in [9] has suggested Nakagami-m fading, a more general yet tractable model. Moreover, different m values can represent mild and deep fading states. Consequently, the LOS (NLOS) states are modeled by large (small) values of m [9]. With this, we use the Nakagami-m model and consider m parameters $m_l \in [1, 2, \ldots, \infty)$ where $l \in \{L, N\}$ denote LOS and NLOS links [9], [12]. If the channel coefficient is $h_l, l \in \{L, N\}$, the power gain $|h_l|^2$ follows a Gamma distribution, i.e., $f_{|h_l|^2}(x) = \frac{m_l^{m_l}}{\Gamma(m_l)} x^{m_l - 1} e^{-m_l x}$, $x > 0$. In our numerical examples, we use large m_L values and small m_N values [9].

With the system model above, the received SNR for a link of length d is given by

$$\text{SNR} = \frac{P\Psi |h_l|^2}{d^{\alpha_l} N_0},$$

where $l \in \{L, N\}$ denote the LOS and NLOS conditions, respectively, $P \in \{P_S, P_R\}$ is the transmit power, $\Psi \triangleq G_{\text{eq}} \mu^2 / (4\pi)^2$ is a constant that includes the directional gain and reference path loss at a 1 m distance with μ being the wavelength of the operating frequency, α_L and α_N are the path loss exponents for LOS and NLOS links, respectively, and N_0 is the noise power.

III. PERFORMANCE ANALYSIS

In this section, we analyze the coverage probability for three modes: (1) direct mode (i.e. no relaying), (2) best relay-selection mode and (3) relaying but no selection. Beam misalignment errors, effect of source and relay power allocation factor, rate coverage and spectral efficiency will be analyzed in Section IV. We make the following two standard assumptions.

1) Only additive noise is considered and co-channel interference is ignored. The noise-limited analysis is realistic because of the high path loss with distance and the narrow mmWave beams [6].
2) We assume that channel state information (CSI) is available at S, D and R so the beam alignment to the desired direction is possible without the need for further beam training. For example, methods in [15] can be used to obtain CSI, and the methods in [14], [39], and [40] can be used to acquire information on direction. Impacts of imperfect CSI and timing overhead associated with initial beam training are beyond the scope of this work and can be potential future research topics. Moreover, to reduce the overhead in practical systems, the search for potential relays can be restricted to a few sectors aligned with the direction of the receiver.

A. DIRECT MODE

When there is no blockage in the $S - D$ link, transmission can occur even without the help of a relay. The direct link can achieve the required SNR or data rate when the $S - D$ distance is short or when the $S - D$ link is not blocked. Using the direct link has the additional benefit of needing only one time slot, compared to the two time slots required in a relay link. Therefore, the analysis of the coverage probability of a direct link is also of great significance.

1) COVERAGE PROBABILITY OF DIRECT LINK

This is defined as the probability that the received SNR exceeds a predefined threshold γ_{th}.

Lemma 1: The coverage probability of the direct link ($S - D$) is given by

$$P_{cov,SD} = p_L(W) P_{SD,L}(\gamma_{\text{th}}) + (1 - p_L(W)) P_{SD,N}(\gamma_{\text{th}}), \quad (1)$$

where $P_{SD,L}(\gamma_{\text{th}})$ and $P_{SD,N}(\gamma_{\text{th}})$ are the conditional coverage probabilities given that the links are in LOS and NLOS conditions, respectively, and are expressed as

$$P_{SD,L}(\gamma_{\text{th}}) = \sum_{n=1}^{m_L} (-1)^{n+1} \binom{m_L}{n} \exp\left(- n a_L W^{\alpha_L} \right) \quad (2)$$

and

$$P_{SD,N}(\gamma_{\text{th}}) = \sum_{n=1}^{m_N} (-1)^{n+1} \binom{m_N}{n} \exp\left(- n a_N W^{\alpha_N} \right), \quad (3)$$

where $a_L = \frac{\eta_L \gamma_{\text{th}} N_0}{P_S \Psi}$, $a_N = \frac{\eta_N \gamma_{th} N_0}{P_S \Psi}$, $\eta_L = m_L (m_L!)^{-\frac{1}{m_L}}$, and $\eta_N = m_N (m_N!)^{-\frac{1}{m_N}}$.

Proof: See Appendix A. □

Remark 1: Lemma 1 provides the coverage probability in terms of LOS and NLOS link coverage using the law of total probability.

B. RELAY SELECTION

When a direct link is not possible due to excessive path loss or blockage, transmission must occur via a relay link. The DF relaying protocol is used and no decoding error is assumed to occur if the received SNR is greater than the threshold γ_{th}. A half duplex relaying operation is adopted, i.e., two time slots are used. During the first time slot, the source sends to the relays. For a potential relay, it can successfully decode the source's message if its received SNR is above the threshold γ_{th}.

In fixed topology AF or DF networks, the optimal relay selection criterion is the maximization of end-to-end SNR [15] or the maximization of the minimum SNR of $S-R$ and $R-D$ links [16]. However, when the relay locations form a PPP, closed-form analysis of these criteria is intractable. Therefore, we consider a slightly suboptimal yet tractable selection strategy with two stages:

- We select a set of relays that can successfully decode the source's message. We refer to this as the decoding set and denote it as $\hat{\Phi}$. This set is a subset of Φ, i.e., the set of relays that can meet the required SNR threshold for decoding. Any node in $\hat{\Phi}$ can retransmit the successfully decoded message to the receiver D. Since the relay's SNR in $S-R$ link highly depends on its distance from S and whether the link is in the LOS or NLOS condition, the decoding set is not uniform in $\mathbb{R}^2$. The spatial distribution of the decoding set is critical to derive coverage probability. We derive this distribution below.
- We next select a relay from the decoding set that has the best link to the receiver, i.e., provides the minimum path loss in $R-D$ link. The closest distance of the selected relay from D is a random variable and we will derive its probability density using Lemma 2.

1) DISTRIBUTION OF DECODING SET OF RELAYS

Mathematically, the decoding set can be defined as

$$\hat{\Phi} = \{x \in \Phi, \text{SNR}_{s,x} \geq \gamma_{\text{th}}\} \tag{4}$$

where s is the location of S, and $\text{SNR}_{s,x}$ is the received SNR of the relay at point $x \in \Phi$. With this rule, a relay located at x in the original point process Φ is included in $\hat{\Phi}$ if the received SNR at x from S is above the predefined threshold γ_{th}. Since $\text{SNR}_{s,x}$ is a function of the distance from x to S, the probability of inclusion in $\hat{\Phi}$ is also a function of x. Specifically, the nodes that are close to S have higher probability of being in the decoding set. Also since $\text{SNR}_{s,x}$ and $\text{SNR}_{s,x'}$ are independent for $x \neq x'$, this selection process is an independent thinning of the original process Φ. However, the thinning probability is not a constant but a function of x. Thus, $\hat{\Phi}$ is an inhomogeneous PPP for which the spatial density of nodes is location dependent. As such, the density of the resultant point process can be written as [35]:

$$\hat{\lambda}(x) = \lambda \mathbb{P}\left(\text{SNR}_{s,x} \geq \gamma_{\text{th}}\right), \tag{5}$$

where $\mathbb{P}(\cdot)$ means probability. The final expression for $\hat{\lambda}(x)$ is given in (6), as shown at the bottom of this page, where $\rho(x)$ is the distance from S to an arbitrary relay R located at x. Since we consider the relays to be distributed in a disc $\mathcal{S}$ of radius $\mathcal{R}$ centered at D (origin), the average number of decoding relays can be obtained as

$$\hat{\Lambda}(\mathcal{S}) = \int_{\mathcal{S}} \hat{\lambda}(x)dx = \int_0^{\mathcal{R}} \int_0^{2\pi} \hat{\lambda}(r,\theta) r d\theta dr, \tag{7}$$

where (r,θ) represents the location x in polar coordinate and in the rest of the paper, we use $\hat{\lambda}(x)$ and $\hat{\lambda}(r,\theta)$ interchangeably. The analysis of coverage requires the distributions of the Euclidean distances from the relays to S and D. Since the path loss is dependent on the distance, use of a polar coordinate to represent the location of a relay is the most convenient for analysis. We set the coordinate axis to be oriented along the line joining the source and receiver so that $\rho(x) = \|x - s\| = \sqrt{r^2 - 2rW\cos\theta + W^2} = \rho(r,\theta)$. The final expression for $\hat{\Lambda}(\mathcal{S})$ is given in (8), as shown at the bottom of the next page. A realization of all nodes, the decoding set, and the selected relay are depicted in Fig. 2.

Since $\hat{\Phi}$ is an inhomogeneous PPP of density $\hat{\lambda}(x)$, we can divide it into two independent processes of densities $p_L(r)\hat{\lambda}(x)$ and $(1-p_L(r))\hat{\lambda}(x)$ to represent the LOS and NLOS sets from the receiver D, respectively. We denote the LOS and NLOS sets as $\hat{\Phi}_L$ and $\hat{\Phi}_N$, respectively.

2) COVERAGE PROBABILITY WITH RELAY SELECTION

Coverage is the probability that the received SNR at the receiver D from the selected relay is above the predefined threshold γ_{th}. Note that we use the same threshold γ_{th} to determine the relays in the decoding set $\hat{\Phi}$ shown in eq. (4). The reason for this is that the equivalent end-to-end SNR of a DF relay is the minimum of two-hop SNRs [41], and setting the same threshold for both links ensures that this

$$\hat{\lambda}(x) = \lambda\Bigg\{p_L(\rho(x)) \sum_{n=1}^{m_L} (-1)^{n+1} \binom{m_L}{n} \exp\left(-na_L\left(\rho(x)\right)^{\alpha_L}\right) + \left(1 - p_L(\rho(x))\right) \sum_{n=1}^{m_N} (-1)^{n+1} \binom{m_N}{n} \exp\left(-na_N\left(\rho(x)\right)^{\alpha_N}\right)\Bigg\}. \tag{6}$$

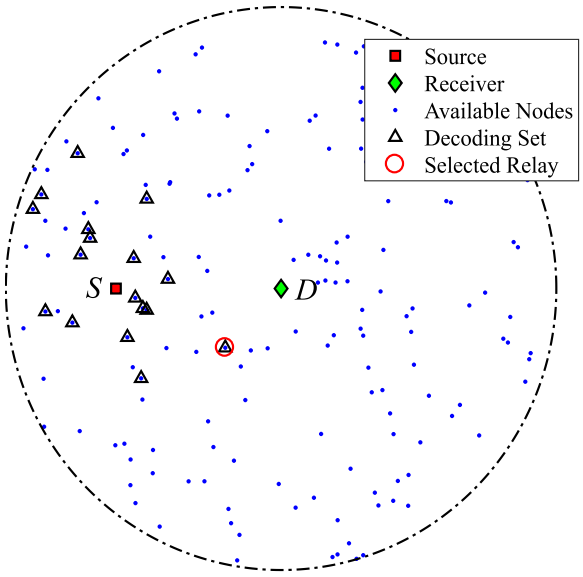

FIGURE 2. One snapshot of relay locations with *S* and *D* as shown. The potential relays (dots) form a PPP. The decoding set is clustered around *S*. Its nodes form an inhomogeneous PPP. In the decoding set, the node with minimum path loss to *D* is selected as the relay.

condition is satisfied. To derive the coverage probability with relay selection, we first need to determine the selected relay. It is the one with the smallest path loss at the receiver in an $R-D$ link. This means the selected relay can only be either the nearest node in $\hat{\Phi}_L$ or the nearest one in $\hat{\Phi}_N$. To derive the coverage probability, we need to know whether a relay from $\hat{\Phi}_L$ or $\hat{\Phi}_N$ is selected, and for that, the distribution of distance of the nearest relays in $\hat{\Phi}_L$ and $\hat{\Phi}_N$ from the receiver are required.

Lemma 2: The complimentary cumulative distribution function (CCDF) of r_L, which is the distance from the receiver to the nearest LOS relay, is given by

$$\bar{F}_{r_L}(z) = \exp\left(-\int_{r=0}^{z}\int_{\theta=0}^{2\pi} p_L(r)\hat{\lambda}(x) r d\theta dr\right), \quad z>0. \quad (9)$$

Proof: The distribution of the distance between the nearest LOS relay from the receiver (at origin) can be derived by utilizing the probability that no LOS relays are in $\mathcal{B}(0,z)$, where $\mathcal{B}(0,z)$ is the ball centered at the origin and with radius z. This is called the void probability for a PPP, and can be written as [35]

$$\begin{aligned}\bar{F}_{r_L}(z) &= \mathbb{P}(r_L > z)\\ &= \mathbb{P}\{\text{no LOS relays in } \mathcal{B}(0,z)\}\\ &= \exp\left(-\Lambda_L([0,z])\right), \end{aligned} \quad (10)$$

where $\Lambda_L([0,z))$ is the mean number of LOS relays in $\mathcal{B}(0,z)$, which can be derived as

$$\Lambda_L([0,z)) = \int_{r=0}^{z}\int_{\theta=0}^{2\pi} p_L(r)\hat{\lambda}(x) r d\theta dr. \quad (11)$$

Substituting (11) in (10), we find the distribution (9). □

Remark 2: Lemma 2 provides an intermediate result to derive the probability density function (PDF) of the distance of the nearest LOS relay from the receiver.

Now, because $f_{r_L}(z) = -\dfrac{d\bar{F}_{r_L}(z)}{dz}$, we find

$$f_{r_L}(z) = z p_L(z)\hat{\lambda}(z,\theta) e^{-\int_{r=0}^{z}\int_{\theta=0}^{2\pi} p_L(z)\hat{\lambda}(x) r d\theta dr}. \quad (12)$$

Similarly, we can derive the CCDF of r_N, which is the distance from the receiver to the nearest NLOS relay, as

$$\bar{F}_{r_N}(z) = \exp\left(-\int_{r=0}^{z}\int_{\theta=0}^{2\pi} (1-p_L(r))\hat{\lambda}(x) r d\theta dr\right), \quad (13)$$

and the corresponding PDF as

$$f_{r_N}(z) = z(1-p_L(z))\hat{\lambda}(z,\theta) e^{-\int_{r=0}^{z}\int_{\theta=0}^{2\pi}(1-p_L(z))\hat{\lambda}(x) r d\theta dr}. \quad (14)$$

By using these distributions of the distance from the receiver to the nearest LOS and NLOS relays, we now derive the probability A_L that an LOS relay will be selected to serve. The selection is based on maximizing the average received power from the candidate relay node or equivalently minimizing the path loss of $R-D$ link.

Lemma 3: The probability that an LOS relay is selected is given by

$$A_L = \int_0^{\infty} \bar{F}_{r_N}\left(z^{\frac{\alpha_L}{\alpha_N}}\right) f_{r_L}(z) dz \quad (15)$$

where $\bar{F}_{r_N}(z)$ is given in (13).

Proof: See Appendix B. □

Remark 3: Lemma 3 gives the probability that the receiver is associated to an LOS or NLOS relay, and is also used to derive the distribution of the distance of a selected relay from the receiver in Lemma 4. This probability is similar to the base station association probabilities in multi-tier and heterogeneous cellular networks [12], but with inhomogeneous PPP distributed base stations. The integral can be computed numerically using tools such as MATLAB.

The probability that an NLOS relay will be used to serve, A_N, is given by

$$A_N = 1 - A_L.$$

$$\hat{\Lambda}(\mathcal{S}) = \lambda\left\{\sum_{n=1}^{m_L}(-1)^{n+1}\binom{m_L}{n}\int_{r=0}^{\mathcal{R}}\int_{\theta=0}^{2\pi} p_L\left(\rho(r,\theta)\right)\exp\left(-n a_L\left(\rho(r,\theta)\right)^{\alpha_L}\right) r d\theta dr + \sum_{n=1}^{m_N}(-1)^{n+1}\binom{m_N}{n}\int_{r=0}^{\mathcal{R}}\int_{\theta=0}^{2\pi}\left(1-p_L\left(\rho(r,\theta)\right)\right)\exp\left(-n a_N\left(\rho(r,\theta)\right)^{\alpha_N}\right) r d\theta dr\right\}. \quad (8)$$

Lemma 4: Given that an LOS relay is selected to serve, the PDF of its distance from the receiver is

$$g_{r_L}(z) = \frac{f_{r_L}(z)}{A_L} \exp\left(-\int_{r=0}^{z^{\frac{\alpha_L}{\alpha_N}}} \int_{\theta=0}^{2\pi} (1 - p_L(r))\hat{\lambda}(x) r d\theta dr\right). \tag{16}$$

Given that an NLOS relay is selected to serve, the PDF of its distance from the receiver is

$$g_{r_N}(z) = \frac{f_{r_N}(z)}{A_N} \exp\left(-\int_{r=0}^{z^{\frac{\alpha_N}{\alpha_L}}} \int_{\theta=0}^{2\pi} p_L(r)\hat{\lambda}(x) r d\theta dr\right). \tag{17}$$

Proof: The proof is given in Appendix C. □

The above lemma enables the computation of coverage probability in the following theorem.

Theorem 1: The overall coverage probability at the receiver using the selected relay is given by

$$P_{cov,SRD} = A_L P_{R,L}(\gamma_{\text{th}}) + A_N P_{R,N}(\gamma_{\text{th}}), \tag{18}$$

where $P_{R,l}(\gamma_{th})$, $l \in \{L, N\}$ is the conditional coverage probability given that a relay from $\hat{\Phi}_l$ is selected, which is given by

$$P_{R,L}(\gamma_{th}) \approx \sum_{k=1}^{m_L} (-1)^{k+1} \binom{m_L}{k} \times \int_{\theta=0}^{2\pi} \int_{z=0}^{\infty} e^{-kb_L z^{\alpha_L}} g_{r_L}(z) z dz d\theta, \tag{19}$$

and

$$P_{R,N}(\gamma_{th}) \approx \sum_{k=1}^{m_N} (-1)^{k+1} \binom{m_N}{k} \times \int_{\theta=0}^{2\pi} \int_{z=0}^{\infty} e^{-kb_N z^{\alpha_N}} g_{r_N}(z) z dz d\theta, \tag{20}$$

where $b_L = \frac{\eta_L \gamma_{th} N_0}{P_R \Psi}$, and $b_N = \frac{\eta_N \gamma_{\text{th}} N_0}{P_R \Psi}$.

Proof: Here we derive the conditional coverage probability when a relay from LOS relays is selected, i.e., the relay from $\hat{\Phi}_L$ closest to the receiver is selected. Thus, coverage can be written as

$$P_{R,L}(\gamma_{\text{th}}) = \mathbb{P}\left(\frac{P_R \Psi |h_L|^2 r_L^{-\alpha_L}}{N_0} > \gamma_{\text{th}}\right) = 1 - \mathbb{P}\left(|h_L|^2 < \frac{\gamma_{\text{th}} N_0 r_L^{\alpha_L}}{P_R \Psi}\right).$$

Now, using a similar approximation to that in (31), we can write

$$P_{R,L}(\gamma_{\text{th}}) \approx \mathbb{E}_{\hat{\Phi}_L}\left[\sum_{k=1}^{m_L} (-1)^{k+1} \binom{m_L}{k} e^{-kb_L r_L^{\alpha_L}}\right] = \sum_{k=1}^{m_L} (-1)^{k+1} \binom{m_L}{k} \times \int_{\theta=0}^{2\pi} \int_{z=0}^{\infty} e^{-kb_L z^{\alpha_L}} g_{r_L}(z) z dz d\theta \tag{21}$$

in which $\mathbb{E}_{\hat{\Phi}_L}[\cdot]$ means expectation over $\hat{\Phi}_L$. Following same steps, we can derive the expression for $P_{R,N}(\gamma_{\text{th}})$ in (20). □

The integrals in (19) and (20) can be numerically evaluated using mathematical tools such as MATLAB.

C. COVERAGE PROBABILITY WITHOUT RELAY SELECTION

The aforementioned best relay selection strategy requires the directional and channel state information either at an end-node or at a central controller to perform the relay selection. Moreover, accurate directional estimation and channel estimation need multiple time-slots and pilot signals, and the signaling and time overhead increase with an increasing number of nodes [14], [15], [39], [40].

Therefore, it may be worthwhile to consider lower-complexity alternatives. To this end, we derive the coverage probability of a simpler scheme that only requires position information of D, which can be readily obtained [42], and picks a relay at random from available nodes that reside in between S and D. This is a trade-off between complexity and performance, because such a relay might perform poorly as it can be in NLOS from S or D with high probability.

Intuitively, picking a relay in between S and D makes $S-R$ and $R-D$ links shorter and results in smaller path loss in each link. Therefore, instead of selecting a relay randomly from entire $\mathcal{S}$ (Fig. 1), we select a relay within a circle centered at the midpoint of S and D and having radius $\mathcal{L}$. The coverage probability at the receiver with such a selection can be written as

$$P_{\text{cov,rand}} = P_{\text{rand},SR} \times P_{\text{rand},RD}, \tag{22}$$

where $P_{\text{rand},SR} = \mathbb{P}(\text{SNR}_{SR} \geq \gamma_{\text{th}})$ and $P_{\text{rand},RD} = \mathbb{P}(\text{SNR}_{RD} \geq \gamma_{\text{th}})$ respectively are the CCDFs of individual link SNRs (i.e., coverage probabilities in $S-R$ and $R-D$ links). The expression for $P_{\text{rand},SR}$ is given by

$$\begin{aligned} P_{\text{rand},SR} = &\sum_{n=1}^{m_L} (-1)^{n+1} \binom{m_L}{n} \frac{1}{2\pi} \\ &\times \int_{\theta=0}^{2\pi} \int_{r=0}^{\mathcal{L}} r e^{-\beta\rho_1} e^{-na_L \rho_1^{\alpha_L}} f_r(r) dr d\theta, \\ &+ \sum_{n=1}^{m_N} (-1)^{n+1} \binom{m_N}{n} \frac{1}{2\pi} \\ &\times \int_{\theta=0}^{2\pi} \int_{r=0}^{\mathcal{L}} r \left(1 - e^{-\beta\rho_1}\right) e^{-na_N \rho_1^{\alpha_N}} f_r(r) dr d\theta, \end{aligned} \tag{23}$$

where $\rho_1 = \sqrt{r^2 + (W/2)^2 - rW\cos\theta}$ is the distance of a randomly selected relay from S, expressions of a_L and a_N are given in Lemma 1, and $f_r(r)$ is the PDF of the distance of a randomly picked relay from the midpoint of the $S-D$ link (note that the midpoint of the $S-D$ link is considered as the origin in this case) and is given by

$$f_r(r) = \frac{2r}{\mathcal{L}^2}, \quad 0 < r < \mathcal{L}. \tag{24}$$

The derivation of (23) follows that of (31) and is omitted. The coverage probability of the $R-D$ link, $P_{\text{rand},RD}$ can

be written similar to (23), with ρ_1 replaced by ρ_2, where $\rho_2 = \sqrt{r^2 + (W/2)^2 + rW\cos\theta}$ is the distance of the randomly picked relay from the receiver, and a_L and a_N replaced by b_L and b_N, respectively, which are given in Theorem 1. In the simulations, unless otherwise stated, we set $\mathcal{L} = W/2$, i.e., we pick a relay from inside a circle centered at midpoint of S and D with diameter W.

IV. SOME EXTENSIONS

A. COVERAGE PROBABILITY WITH BEAM ALIGNMENT ERRORS

Up until now, we have assumed perfect beam alignment, and thus coverage probabilities (1) and (18) are derived without considering beam alignment errors. Next we investigate the effect of beam alignment errors on coverage probability.

We use the analytical method given in [12]. For an $S-D$, $S-R$, or $R-D$ link, let ε denote the beam alignment error, which follows a Gaussian distribution with zero mean and variance σ^2. Thus, CDF of $|\varepsilon|$ (absolute value of the error) is expressed as $F_{|\varepsilon|}(x) = \text{erf}\left(x/(\sqrt{2}\sigma)\right)$, where erf$(\cdot)$ is the Gaussian error function. Denote PDF of the effective antenna gain $G_{\text{eq},SD}$, $G_{\text{eq},SR}$ and $G_{\text{eq},RD}$ for the $S-D$, $S-R$ and $R-D$ links as $f_{G_{\text{eq},SD}}(y)$, $f_{G_{\text{eq},SR}}(y)$ and $f_{G_{\text{eq},RD}}(y)$, respectively. Thus, $f_{G_{\text{eq},SD}}(y)$, $f_{G_{\text{eq},SR}}(y)$ and $f_{G_{\text{eq},RD}}(y)$ all have the same expression given as

$$F_{|\varepsilon|}\left(\frac{\phi}{2}\right)^2 \delta_{(y-G_{\max}^2)} + 2F_{|\varepsilon|}\left(\frac{\phi}{2}\right)\left(1 - F_{|\varepsilon|}\left(\frac{\phi}{2}\right)\right) \times \delta_{(y-G_{\max}G_{\min})} + \left(1 - F_{|\varepsilon|}\left(\frac{\phi}{2}\right)\right)^2 \delta_{(y-G_{\min}^2)}, \quad (25)$$

where $\delta_{(\cdot)}$ is the Kronecker delta function.

1) ERROR IN DIRECT LINK

Since the coverage probability (1) depends on the effective antenna gain $G_{\text{eq},SD}$ of the $S-D$ link, total $P_{\text{cov},SD}$ can be computed by averaging over $f_{G_{\text{eq},SD}}(y)$ as follows [12]:

$$\begin{aligned} P_{\text{cov},SD} &= \int_0^\infty P_{\text{cov},SD}(y) f_{G_{\text{eq},SD}}(y) dy \\ &= F_{|\varepsilon|}(\phi/2)^2 P_{\text{cov},SD}(G_{\max}^2) + 2F_{|\varepsilon|}(\phi/2)\bar{F}_{|\varepsilon|}(\phi/2) \\ &\quad \times \mathrm{P}_{\text{cov,SD}}(G_{\max}G_{\min}) + \bar{F}_{|\epsilon|}(\phi/2)^2 P_{\text{cov},SD}(G_{\min}^2) \end{aligned} \quad (26)$$

where $P_{\text{cov},SD}(y)$ refers to the coverage probability (1) as a function of effective antenna gain y of $S-D$ link, and $\bar{F}_{|\varepsilon|}(\cdot) \triangleq 1 - F_{|\varepsilon|}(\cdot)$.

2) ERROR USING RELAYS

It is reasonable to assume that the beam alignment errors in the $S-R$ and $R-D$ links are independent. Thus, the overall coverage probability $P_{\text{cov},SRD}$ by using the selected relay is given by [25]

$$\begin{aligned} &P_{\text{cov},SRD} \\ &= \int_0^\infty \int_0^\infty \mathrm{P}_{\text{cov},SRD}(y_1, y_2) f_{G_{\text{eq},SR}}(y_1) f_{G_{\text{eq},RD}}(y_2) dy_1 dy_2 \\ &= F_{|\varepsilon|}(\phi/2)^4 P_{\text{cov},SRD}\left(G_{\max}^2, G_{\max}^2\right) \\ &\quad + 2F_{|\varepsilon|}(\phi/2)^3 \bar{F}_{|\varepsilon|}(\phi/2) P_{\text{cov},SRD}\left(G_{\max}^2, G_{\max}G_{\min}\right) \\ &\quad + F_{|\varepsilon|}(\phi/2)^2 \bar{F}_{|\varepsilon|}(\phi/2)^2 P_{\text{cov},SRD}\left(G_{\max}^2, G_{\min}^2\right) \\ &\quad + 2F_{|\varepsilon|}(\phi/2)^3 \bar{F}_{|\varepsilon|}(\phi/2) P_{\text{cov},SRD}\left(G_{\max}G_{\min}, G_{\max}^2\right) \\ &\quad + 4F_{|\varepsilon|}(\phi/2)^2 \bar{F}_{|\varepsilon|}(\phi/2)^2 P_{\text{cov},SRD}\left(G_{\max}G_{\min}, G_{\max}G_{\min}\right) \\ &\quad + 2F_{|\varepsilon|}(\phi/2) \bar{F}_{|\varepsilon|}(\phi/2)^3 P_{\text{cov},SRD}\left(G_{\max}G_{\min}, G_{\min}^2\right) \\ &\quad + F_{|\varepsilon|}(\phi/2)^2 \bar{F}_{|\varepsilon|}(\phi/2)^2 P_{\text{cov},SRD}\left(G_{\min}^2, G_{\max}^2\right) \\ &\quad + 2F_{|\varepsilon|}(\phi/2) \bar{F}_{|\varepsilon|}(\phi/2)^3 P_{\text{cov},SRD}\left(G_{\min}^2, G_{\max}G_{\min}\right) \\ &\quad + \bar{F}_{|\varepsilon|}(\phi/2)^4 P_{\text{cov},SRD}\left(G_{\min}^2, G_{\min}^2\right), \end{aligned} \quad (27)$$

where $P_{\text{cov},SRD}(y_1, y_2)$ means the coverage probability (18) as a function of y_1 (the effective antenna gain of the $S-R$ link) and y_2 (the effective antenna gain of the $R-D$ link).

B. EFFECT OF POWER ALLOCATION FACTOR

Let the total transmit power of the system be P_T. We study the effect of dividing up P_T between the source and the relay. To this end, we define a power factor $\xi = \dfrac{P_S}{P_S + P_R}$. With this, we allocate the power of $P_S = \xi P_T$ to the source and $P_R = (1-\xi)P_T$ to the selected relay.

C. RATE COVERAGE PROBABILITY

Rate coverage refers to the probability that the achievable link rate is greater than or equal to the rate threshold $\Gamma_{\text{th}} > 0$. Since the rate gives a true measure of data bits received per second at the receiver, it is a critical performance metric, indicating the quality of the link. Moreover, the use of mmWave frequency is fundamentally motivated by achieving higher rates and knowing that the rate coverage provides a quantitative performance measure for these systems. The achievable rate using the relay can be written as

$$\Gamma = \frac{B}{2}\log_2(1 + \text{SNR}), \quad (28)$$

where the factor of $1/2$ is used because two time slots are required for a complete transmission using a relay, and B is the bandwidth assigned to the system.

Lemma 5: The rate coverage probability $\mathbb{P}(\Gamma > \Gamma_{th})$ of a relay transmission is given by

$$P_{\text{cov,Rate}} = P_{\text{cov}}\left(2^{\frac{2\Gamma_{\text{th}}}{B}} - 1\right) \quad (29)$$

where $P_{\text{cov}}(\gamma_{\text{th}})$ is the coverage probability in (18) *or* (22) *as a function of SNR threshold γ_{th}.*

Proof: The expression is obtained straightforwardly by manipulating (28) and is omitted here. □

Remark 4: The rate coverage for the direct link is given by $P_{\text{cov,Rate}} = P_{\text{cov}}\left(2^{\frac{\Gamma_{\text{th}}}{B}} - 1\right)$ due to the use of single time slot for S to D transmission, and $P_{\text{cov}}(\gamma_{\text{th}})$ is the coverage probability in (1) *as a function of SNR threshold γ_{th}.*

D. SPECTRAL EFFICIENCY

The spectral efficiency can be defined as the throughput of a given link per hertz of bandwidth, and for two-hop transmission it can be written as [31],

$$\mathrm{SE} = \frac{1}{2} P_{\mathrm{cov}}(\gamma_{\mathrm{th}}) \log_2(1+\gamma_{\mathrm{th}}), \tag{30}$$

where the factor of $1/2$ is due to the use of two time slots when relaying is used. To make a fair comparison, we do not use this factor in calculating the spectral efficiency of the direct link.

TABLE 1. Simlation parameters.

Notation	Parameter	Value
P_S	Source transmit power	30 dBm
P_R	Relay transmit power	30 dBm
$\mathcal{R}$	Radius of the simulation area	1000 m
f	Operating frequency	28 GHz
B	System bandwidth	1 GHz
α_L, α_N	LOS and NLOS path loss exponents	2, 3.3 [7]
m_L, m_N	Nakagami-m parameters for LOS and NLOS cases	3, 2 [9]
$G_{\max}, G_{\min}$	Main lobe and side lobe gains	18 dBi, -10 dBi
ϕ	Half power beamwidth	30°
σ	Beam alignment error	$0^\circ, 5^\circ, 8^\circ, 10^\circ$
β	Blockage parameter	0.0095 [33]
N_0	Noise power	-174 dBm/Hz + $10\log_{10}(B)+10$ dB

V. SIMULATION AND ANALYTICAL RESULTS

We next validate our analysis by comparing the analytical results with Monte Carlo simulations. Each simulation runs over 10^5 independent network realizations. Table 1 shows the simulation parameters unless otherwise specified. In the figures, the curves represent the analytical results and the markers denote simulations. Overall, the analytical results closely match the simulations, thereby verifying the correctness of our analysis.

Fig. 3 plots the average number of relays in the decoding set (8) which meet the required SNR threshold for different relay densities. These relays are capable of decoding the source's message and forwarding it to the receiver. The locations of these relays form an inhomogeneous PPP with density (6). As expected, when the required SNR threshold increases, the decoding relay number decreases. This is because only the relays which are closer to S and fall in LOS region from S may achieve the required SNR threshold. For example, for a moderate relay density of 100 relays per km^2, seven nodes can act as decoding relays at an SNR threshold of 20 dB. The coverage at the receiver is contributed by the best relay from this decoding set, and having a greater number of relays in this set increases the probability of coverage.

Fig. 4 plots the association probability versus SNR thresholds for two sets of relay densities. This is the probability

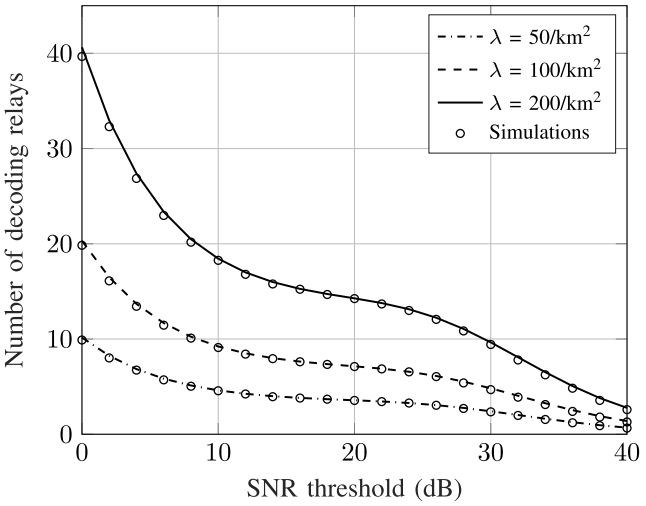

FIGURE 3. Number of decoding relay nodes versus SNR threshold for different relay densities when $W = 300$ meters.

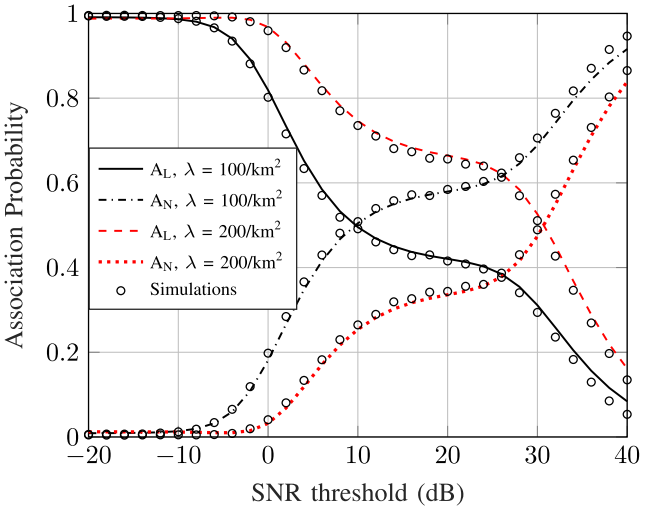

FIGURE 4. Association probability of the receiver (D) with LOS and NLOS relays for different relay densities for $W = 300$ m.

whether a relay is selected from $\hat{\Phi}_L$ or from $\hat{\Phi}_N$ in the second link. As we can see, association to an LOS relay decreases with an increase in SNR threshold (γ_{th}) and the trend is opposite for the NLOS relays. The reason is as follows: for a high SNR threshold, the nodes which are very close to S act as the decoding set, which are most likely to fall in NLOS range from D according to the negative exponential blockage model. We also observe that LOS association probability is higher for higher relay densities, as the chance of more LOS relays improves with an increased total number of relays.

Fig. 5 plots and compares the coverage without relaying in (1), random relay in (22), and with relay selection in (18) when $S-D$ distance W is set to 300 meters. While coverage improves slightly with random relay compared to the direct link, relay selection confers dramatic improvements. Since at this distance the direct link is unlikely to be LOS, its coverage probability remains close to 5% for the practical

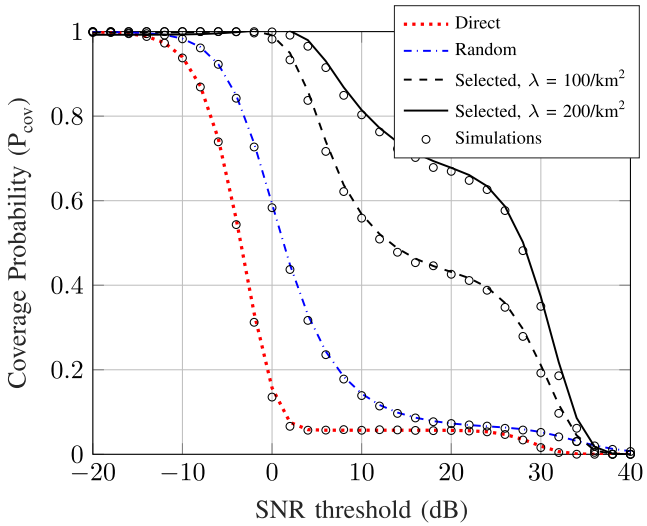

FIGURE 5. **Coverage probability vs. SNR thresholds with direct link, relay selection and random relay for different relay densities when $W = 300$ m.**

range of SNR thresholds ($2 - 24$ dB). With relay selection, it improves drastically, for example 57% with 100 relays/km^2 and 80% with 200 relays/km^2 at $\gamma_{\text{th}} = 10$ dB. Also we observe significant coverage improvement with increasing relay density. For example, when the density doubles from 100 to 200 relays/km^2, coverage increases from 43% to more than 68% for $\gamma_{\text{th}} = 20$ dB. The coverage for the randomly picked relay appears equal for $\lambda = 100/\text{km}^2$ and $200/\text{km}^2$ due to the fact that both densities lead to a negligible probability that the number of relay nodes inside the selection region is zero, which is the void probability for a PPP (given by $e^{-\lambda\pi\mathcal{L}^2}$) [35]. Once a relay is present inside the selection region, coverage due to random selection is independent of density of relays due to the node locations being independent and uniformly distributed in the region [25].

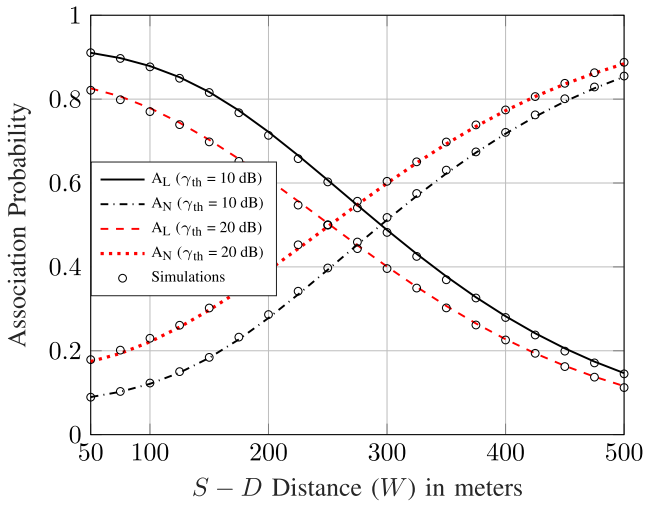

FIGURE 6. **Association probability of the receiver (D) with LOS and NLOS relays versus the $S - D$ distance W ($\lambda = 100/\text{km}^2$).**

Fig. 6 plots the association probability of LOS and NLOS relays versus $S - D$ distance for two sets of SNR thresholds. As shown in the figure, LOS association probability slightly decreases when γ_{th} changes from 10 dB to 20 dB. This is because there is a larger number of decoding relays available at lower SNR thresholds, and this provides better coverage. In both cases, as the receiver moves farther from the source, LOS association probability decreases. This is expected since for a fixed SNR threshold, the average number of decoding relays is fixed and those relays are located near S. This means the distance between decoding relays and the receiver increases with increasing W, consequently decreasing the probability that the $R - D$ link is in LOS. From this we can conclude that when the separation starts to increase, NLOS relays in the $R-D$ link play a major role in providing coverage to the receiver.

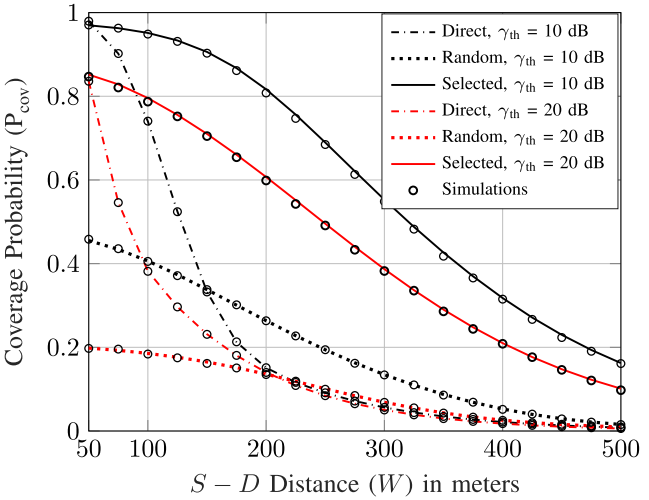

FIGURE 7. **Coverage probability versus W for different SNR thresholds, $\lambda = 100/\text{km}^2$.**

Fig. 7 plots and compares the coverage probability of the direct link, a randomly chosen relay and the selected relay versus the $S - D$ separation distance W. Note that the coverage probabilities decrease with increasing distance, and this is mainly due to blockage and path losses which increase with increasing distance. Also, we observe that, compared to direct link, the coverage is significantly improved when relay selection is used. For example, when $S - D$ distance is 200 meters, the coverage probability increases from 15% to more than 60% and 80% for 20 dB and 10 dB SNR thresholds, respectively. As we can see, the only time that direct link coverage probability becomes similar to that with relay selection is when W is 50 meters. This is because, for the shorter links, the chance of blockage in $S - D$ link is small and there is a high probability that the $S - D$ link is in the LOS condition and has very small path loss. The random relay is picked from a disc centered at the midpoint of S and D and with radius 150 meters.[1] This relay offers a lower coverage compared to the direct link up to a distance

[1]The purpose of this setting is to have a higher chance that there is at least one relay in the selection region.

of 150 meters when $\gamma_{\text{th}} = 10$ dB, and it only provides a small coverage gain for $W > 150$ meters. For a higher SNR threshold of $\gamma_{\text{th}} = 20$ dB, the coverage remains less than 20% for the entire range of W. Therefore, simple random selection strategy is not promising to improve the coverage, which further signifies the role of relay selection in the proposed network.

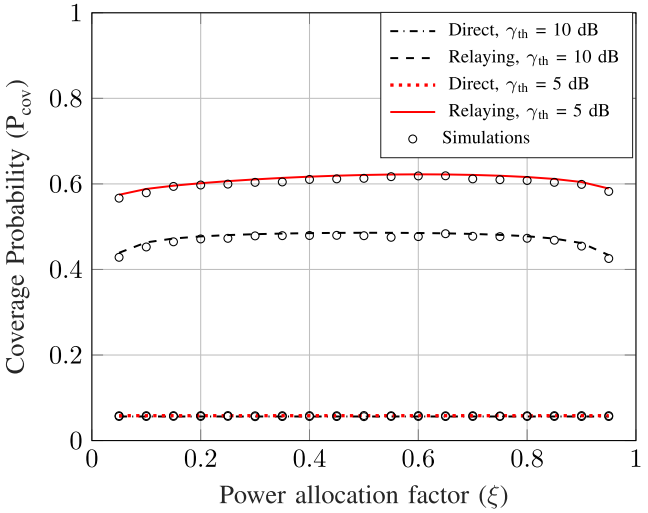

FIGURE 8. Coverage probability versus ξ for different SNR thresholds ($W = 300$ m, $\lambda = 100/\text{km}^2$).

In Fig. 8, we plot the effect of the power allocation factor $\xi = \frac{P_S}{P_T}$ on the coverage probability of the direct link and selected relay when W is set to 300 meters for different SNR thresholds. The total power P_T is divided between the source and relay as $P_S = \xi P_T$ and $P_R = (1-\xi)P_T$, where ξ varies from 0.05 up to 0.95. As expected, we observe higher coverage for lower SNR thresholds when relays are deployed. The coverage probability for a direct link has a negligible difference for different γ_{th} and remains unchanged for the entire range of ξ. This is because of the fact that at an $S-D$ distance of 300 meters, the LOS probability of the link is very small and fixed but dominates the overall coverage. Using relays, the optimal coverage for both SNR thresholds is observed at $\xi = 0.5$, i.e., when the power is equally divided between the source and the relay.

To study the effect of beam alignment errors on overall coverage probability, we plot the coverage for different values of beam alignment errors in Fig. 9. When λ is $200/\text{km}^2$ and $W = 300$ meters, we observe a negligible change in coverage when σ is up to 5 degrees. When σ reaches 8° and above, the coverage begins to drop for both the direct link and the relay aided link.

In Fig. 10, we plot the rate coverage probability, which gives the measure of achievable rate of our system. We plot the rate coverage for two densities of $100/\text{km}^2$ and $200/\text{km}^2$ versus the rate threshold in Gbps and observe that the selected relay provides a higher rate coverage for rate regions up to 5.8 and 6 Gbps, respectively. Despite the need for two time

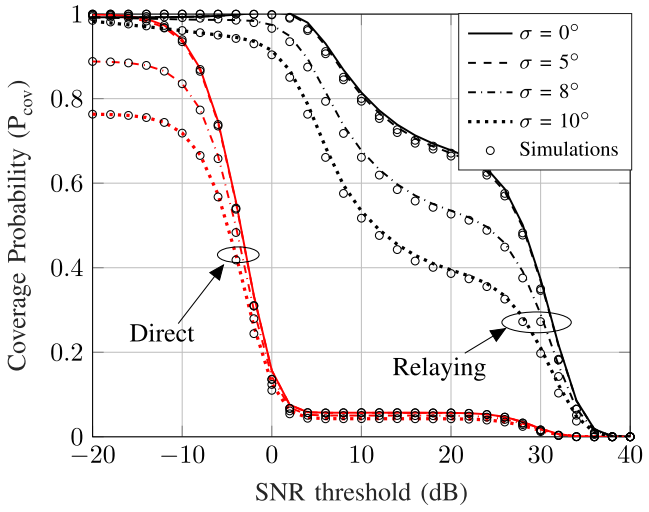

FIGURE 9. Coverage Probability versus SNR threshold for different beamforming errors when $\lambda = 200/\text{km}^2$ and $W = 300$ m.

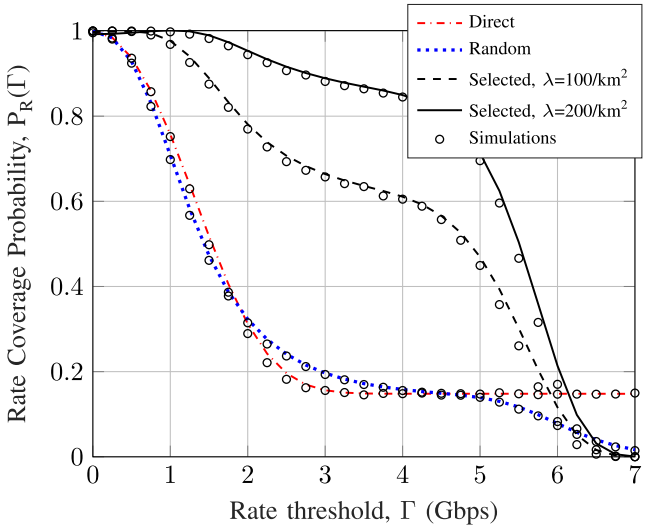

FIGURE 10. Rate Coverage versus rate threshold for different relay densities when $W = 200$ m.

slots when using a relay link, which halves the achievable rate, relay selection achieves better rate coverage. However, for a very high rate threshold in the range of $6-12$ Gbps (although plotted only up to 7 Gbps in Fig. 10), the direct link provides better coverage. The randomly picked relay provides slightly higher rate coverage in the rate regions between 2 and 4 Gbps compared to the direct link but the coverage is significantly smaller than that with relay selection.

Fig. 11 plots the system spectral efficiency shown in (30). As we can see, the spectral efficiency is significantly higher with relay selection when compared to the direct link and randomly picked relay. As well, the spectral efficiency improves notably when increasing the relay density. Specifically, at a 20 dB SNR threshold, the spectral efficiency improves from about 1.5 bps/Hz to 2.25 bps/Hz (i.e., 50% improvement) when increasing relay density from $100/\text{km}^2$ to $200/\text{km}^2$. The peaks occur close to 24 dB SNR threshold in most

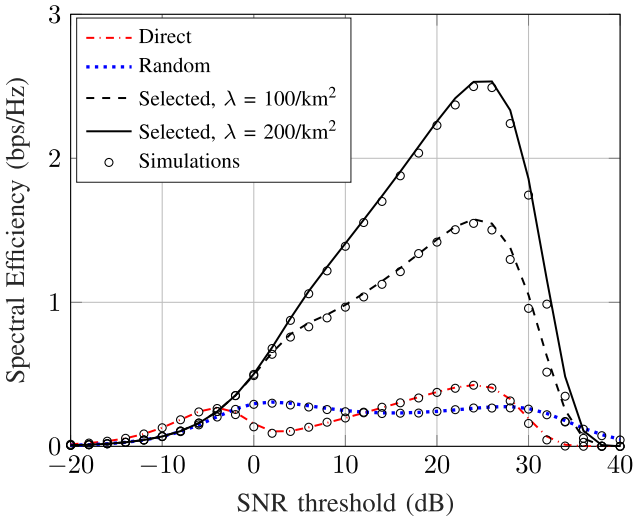

FIGURE 11. Spectrum Efficiency versus SNR threshold for different relay densities when $W = 300$ m.

cases which suggests that setting this optimal SNR threshold provides the best spectral efficiency.

VI. CONCLUSION

DF relaying in mmWave bands has not been analyzed before. In this paper, we therefore analyzed coverage probability of such a network using tools and models from stochastic geometry. Specifically, the relay locations were modeled as a PPP. All the fundamental mmWave features including blockage, path loss, and directional gain were considered. We analyzed the direct link, best relay selection and random choice of a relay. The analysis of best relay selection is the most demanding. To this end, we first derived the distribution of the decoding set as an inhomogeneous PPP, and derived the statistical distribution of the distance of the relay which provides the minimum path loss to the receiver. We also derived the coverage probability with random relay (e.g., non selection). We also extended our analysis to study the effect of beam alignment errors, the effect of power splitting, rate coverage probability, and spectral efficiency. Some of the observations are as follows:

1) We show that the relay deployment provides a significant coverage improvement. For example, at an SNR threshold of 10 dB, coverage improves from 5% without relays to 57% with relay selection for a relay deployment density of $100/\text{km}^2$.
2) When a randomly picked relay is used, i.e., without selection, a slight improvement in coverage performance compared to direct link is achieved. However, the coverage probability with such a selection is considerably smaller than that with the best relay selection, signifying the importance of an appropriate relay selection method.
3) In addition, mmWave DF relay deployment is shown to provide significant performance gains in terms of rate coverage and spectral efficiency compared to direct communication.

For future work, performance evaluation considering the effect of co-channel interference on the considered relay network will be conducted. Moreover, including the effect of imperfect channel and directional information will be an interesting topic of future research.

APPENDIX A
PROOF OF LEMMA 1

Equation (1) is obtained using the law of total probability, where $p_L(W)$ and $1 - p_L(W)$ represent the LOS and NLOS probabilities for a link of distance W. We next derive the conditional coverage probability $P_{SD,L}(\gamma_{\text{th}})$, which is the probability that $\text{SNR}_{SD,L}$ (SNR of the $S - D$ link when it is in LOS condition) is above the predefined threshold γ_{th}, as follows.

$$\begin{aligned} P_{SD,L}(\gamma_{\text{th}}) &= \mathbb{P}\left(\text{SNR}_{SD,L} > \gamma_{\text{th}}\right) \\ &= \mathbb{P}\left(\frac{P_S \Psi |h_L|^2 \, W^{-\alpha_L}}{N_0} > \gamma_{\text{th}}\right) \\ &= 1 - \mathbb{P}\left(|h_L|^2 < \frac{\gamma_{\text{th}} N_0 W^{\alpha_L}}{P_S \Psi}\right) \\ &\overset{(a)}{\approx} 1 - \left(1 - \exp\left(-\frac{\eta_L \gamma_{\text{th}} N_0 W^{\alpha_L}}{P_S \Psi}\right)\right)^{m_L} \\ &= \sum_{n=1}^{m_L} (-1)^{n+1} \binom{m_L}{n} \exp\left(-n a_L W^{\alpha_L}\right), \end{aligned} \tag{31}$$

where the approximation (a) is used similar to that in [9] for the normalized gamma random variable and the final step follows from the binomial expansion.

Similarly, we can derive $P_{SD,N}(\gamma_{\text{th}})$ as shown in (3).

APPENDIX B
PROOF OF LEMMA 3

The nearest LOS relay is selected if it provides smaller path loss than that from the nearest NLOS relay, i.e.,

$$\begin{aligned} A_L &\triangleq \mathbb{P}\left(P_R \Psi r_L^{-\alpha_L} > P_R \Psi r_N^{-\alpha_N}\right) \\ &= \mathbb{P}\left(r_N > r_L^{\left(\frac{\alpha_L}{\alpha_N}\right)}\right) \\ &= \int_0^\infty \mathbb{P}\left(r_N > r_L^{\left(\frac{\alpha_L}{\alpha_N}\right)} | r_L = z\right) f_{r_L}(z) dz \\ &= \int_0^\infty \bar{F}_{r_N}\left(z^{\left(\frac{\alpha_L}{\alpha_N}\right)}\right) f_{r_L}(z) dz, \end{aligned} \tag{32}$$

where $\bar{F}_{r_N}(z)$ is given in (13).

APPENDIX C
PROOF OF LEMMA 4

The CCDF of the distance from the receiver to the selected relay conditioned on a relay from $\hat{\Phi}_L$ being selected can be written as

$$\bar{G}_{r_L}(z) = \mathbb{P}\Big(\text{No LOS relay is closer than } z \text{ given that no NLOS relay is closer than } r_L^{\frac{\alpha_L}{\alpha_N}}\Big)$$

$$= \mathbb{P}\left(r_L > z | r_N > r_L^{\left(\frac{\alpha_L}{\alpha_N}\right)}\right)$$
$$= \frac{\int_z^\infty \mathbb{P}\left(r_N > r_L^{\left(\frac{\alpha_L}{\alpha_N}\right)} | r_L = v\right) f_{r_L}(v) dv}{\mathbb{P}\left(r_N > r_L^{\left(\frac{\alpha_L}{\alpha_N}\right)}\right)}$$
$$\stackrel{(b)}{=} \frac{\int_z^\infty \exp\left(-\Lambda_N\left([0, v^{\frac{\alpha_L}{\alpha_N}})\right)\right) f_{r_L}(v) dv}{A_L}, \quad (33)$$

where in (b) we use the void probability for PPP $\hat{\Phi}_N$, where $\Lambda_N([0, v^{\frac{\alpha_L}{\alpha_N}})) = \int_{r=0}^{v^{\left(\frac{\alpha_L}{\alpha_N}\right)}} \int_{\theta=0}^{2\pi} (1 - p_L(r))\, \hat{\lambda}(x) r d\theta dr$ is the expected number of NLOS relays in $\mathcal{B}(0, v^{\frac{\alpha_L}{\alpha_N}})$. Now, the required distance distribution in (16) is obtained using $g_{r_L}(z) = -\frac{d\bar{G}_{r_L}(z)}{dz}$. The derivation for $g_{r_N}(z)$ in (17) follows similarly.

ACKNOWLEDGMENT

This paper was presented in part at the IEEE International Conference on Communications, Kansas City, Missouri, USA, May 2018.

REFERENCES

[1] Z. Pi and F. Khan, "An introduction to millimeter-wave mobile broadband systems," *IEEE Commun. Mag.*, vol. 49, no. 6, pp. 101–107, Jun. 2011.
[2] W. Roh *et al.*, "Millimeter-wave beamforming as an enabling technology for 5G cellular communications: Theoretical feasibility and prototype results," *IEEE Commun. Mag.*, vol. 52, no. 2, pp. 106–113, Feb. 2014.
[3] C.-X. Wang *et al.*, "Cellular architecture and key technologies for 5G wireless communication networks," *IEEE Commun. Mag.*, vol. 52, no. 2, pp. 122–130, Feb. 2014.
[4] T. Kim, J. Park, J.-Y. Seol, S. Jeong, J. Cho, and W. Roh, "Tens of Gbps support with mmwave beamforming systems for next generation communications," in *Proc. IEEE Globecom*, Dec. 2013, pp. 3685–3690.
[5] F. Boccardi, R. W. Heath, A. Lozano, T. L. Marzetta, and P. Popovski, "Five disruptive technology directions for 5G," *IEEE Commun. Mag.*, vol. 52, no. 2, pp. 74–80, Feb. 2014.
[6] T. S. Rappaport *et al.*, "Millimeter wave mobile communications for 5G cellular: It will work!" *IEEE Access*, vol. 1, pp. 335–349, May 2013.
[7] M. R. Akdeniz *et al.*, "Millimeter wave channel modeling and cellular capacity evaluation," *IEEE J. Sel. Areas Commun.*, vol. 32, no. 6, pp. 1164–1179, Jun. 2014.
[8] S. Rangan, T. S. Rappaport, and E. Erkip, "Millimeter-wave cellular wireless networks: Potentials and challenges," *Proc. IEEE*, vol. 102, no. 3, pp. 366–385, Mar. 2014.
[9] T. Bai and R. W. Heath, Jr., "Coverage and rate analysis for millimeter-wave cellular networks," *IEEE Trans. Wireless Commun.*, vol. 14, no. 2, pp. 1100–1114, Feb. 2015.
[10] S. Singh, M. N. Kulkarni, A. Ghosh, and J. G. Andrews, "Tractable model for rate in self-backhauled millimeter wave cellular networks," *IEEE J. Sel. Areas Commun.*, vol. 33, no. 10, pp. 2196–2211, Oct. 2015.
[11] J. G. Andrews, T. Bai, M. N. Kulkarni, A. Alkhateeb, A. K. Gupta, and R. W. Heath, Jr., "Modeling and analyzing millimeter wave cellular systems," *IEEE Trans. Commun.*, vol. 65, no. 1, pp. 403–430, Jan. 2017.
[12] E. Turgut and M. C. Gursoy, "Coverage in heterogeneous downlink millimeter wave cellular networks," *IEEE Trans. Commun.*, vol. 65, no. 10, pp. 4463–4477, Oct. 2017.
[13] A. Thornburg, T. Bai, and R. W. Heath, Jr., "Performance analysis of outdoor mmWave ad hoc networks," *IEEE Trans. Signal Process.*, vol. 64, no. 15, pp. 4065–4079, Aug. 2016.
[14] M. Giordani, M. Mezzavilla, and M. Zorzi, "Initial access in 5G mmWave cellular networks," *IEEE Commun. Mag.*, vol. 54, no. 11, pp. 40–47, Nov. 2016.
[15] S. Atapattu, Y. Jing, H. Jiang, and C. Tellambura, "Relay selection and performance analysis in multiple-user networks," *IEEE J. Sel. Areas Commun.*, vol. 31, no. 8, pp. 1517–1529, Aug. 2013.
[16] S. S. Ikki and M. H. Ahmed, "Performance analysis of adaptive decode-and-forward cooperative diversity networks with best-relay selection," *IEEE Trans. Commun.*, vol. 58, no. 1, pp. 68–72, Jan. 2010.
[17] D. Senaratne and C. Tellambura, "Unified exact performance analysis of two-hop amplify-and-forward relaying in Nakagami fading," *IEEE Trans. Veh. Technol.*, vol. 59, no. 3, pp. 1529–1534, Mar. 2010.
[18] G. Amarasuriya, M. Ardakani, and C. Tellambura, "Output-threshold multiple-relay-selection scheme for cooperative wireless networks," *IEEE Trans. Veh. Technol.*, vol. 59, no. 6, pp. 3091–3097, Jul. 2010.
[19] V. N. Q. Bao, T. Q. Duong, and C. Tellambura, "On the performance of cognitive underlay multihop networks with imperfect channel state information," *IEEE Trans. Commun.*, vol. 61, no. 12, pp. 4864–4873, Dec. 2013.
[20] X. Gong, S. A. Vorobyov, and C. Tellambura, "Joint bandwidth and power allocation with admission control in wireless multi-user networks with and without relaying," *IEEE Trans. Signal Process.*, vol. 59, no. 4, pp. 1801–1813, Apr. 2011.
[21] S. Singh, F. Ziliotto, U. Madhow, E. M. Belding, and M. Rodwell, "Blockage and directivity in 60 GHz wireless personal area networks: From cross-layer model to multihop MAC design," *IEEE J. Sel. Areas Commun.*, vol. 27, no. 8, pp. 1400–1413, Jun. 2009.
[22] V. Sakarellos, D. Skraparlis, A. D. Panagopoulos, and J. D. Kanellopoulos, "Optimum placement of radio relays in millimeter-wave wireless dual-hop networks," *IEEE Antennas Propag. Mag.*, vol. 51, no. 2, pp. 190–199, Apr. 2009.
[23] S. Biswas, S. Vuppala, J. Xue, and T. Ratnarajah, "On the performance of relay aided millimeter wave networks," *IEEE J. Sel. Topics Signal Process.*, vol. 10, no. 3, pp. 576–588, Apr. 2016.
[24] S. Wu, R. Atat, N. Mastronarde, and L. Liu, "Coverage analysis of D2D relay-assisted millimeter-wave cellular networks," in *Proc. IEEE WCNC*, Mar. 2017, pp. 1–6.
[25] K. Belbase, C. Tellambura, and H. Jiang, "Two-way relay selection for millimeter wave networks," *IEEE Commun. Lett.*, vol. 22, no. 1, pp. 201–204, Jan. 2018.
[26] J. G. Andrews, F. Baccelli, and R. K. Ganti, "A tractable approach to coverage and rate in cellular networks," *IEEE Trans. Commun.*, vol. 59, no. 11, pp. 3122–3134, Nov. 2011.
[27] H. Wang, S. Ma, and T.-S. Ng, "On performance of cooperative communication systems with spatial random relays," *IEEE Trans. Commun.*, vol. 59, no. 4, pp. 1190–1199, Apr. 2011.
[28] H. Wang, S. Ma, T.-S. Ng, and H. V. Poor, "A general analytical approach for opportunistic cooperative systems with spatially random relays," *IEEE Trans. Wireless Commun.*, vol. 10, no. 12, pp. 4122–4129, Dec. 2011.
[29] Y. Dhungana and C. Tellambura, "Outage probability of underlay cognitive relay networks with spatially random nodes," in *Proc. IEEE Globecom*, Dec. 2014, pp. 3597–3602.
[30] A. Behnad, A. M. Rabiei, and N. C. Beaulieu, "Performance analysis of opportunistic relaying in a Poisson field of amplify-and-forward relays," *IEEE Trans. Commun.*, vol. 61, no. 1, pp. 97–107, Jan. 2013.
[31] Z. Lin, Y. Li, S. Wen, Y. Gao, X. Zhang, and D. Yang, "Stochastic geometry analysis of achievable transmission capacity for relay-assisted device-to-device networks," in *Proc. IEEE ICC*, Jun. 2014, pp. 2251–2256.
[32] W. Lu and M. Di Renzo, "Performance evaluation of relay-aided cellular networks by using stochastic geometry," in *Proc. 19th IEEE CAMAD Workshop*, Dec. 2014, pp. 265–269.
[33] T. Bai, R. Vaze, and R. W. Heath, Jr., "Analysis of blockage effects on urban cellular networks," *IEEE Trans. Wireless Commun.*, vol. 13, no. 9, pp. 5070–5083, Sep. 2014.
[34] T. S. Rappaport, G. R. Maccartney, M. K. Samimi, and S. Sun, "Wideband millimeter-wave propagation measurements and channel models for future wireless communication system design," *IEEE Trans. Commun.*, vol. 63, no. 9, pp. 3029–3056, Sep. 2015.
[35] S. N. Chiu, D. Stoyan, W. S. Kendall, and J. Mecke, *Stochastic Geometry and its Applications*. Hoboken, NJ, USA: Wiley, 2013.
[36] G. R. MacCartney, J. Zhang, S. Nie, and T. S. Rappaport, "Path loss models for 5G millimeter wave propagation channels in urban microcells," in *Proc. IEEE Globecom*, Dec. 2013, pp. 3948–3953.

[37] M. Di Renzo, "Stochastic geometry modeling and analysis of multi-tier millimeter wave cellular networks," *IEEE Trans. Wireless Commun.*, vol. 14, no. 9, pp. 5038–5057, Sep. 2015.
[38] M. Ding, P. Wang, D. López-Pérez, G. Mao, and Z. Lin, "Performance impact of LoS and NLoS transmissions in dense cellular networks," *IEEE Trans. Wireless Commun.*, vol. 15, no. 3, pp. 2365–2380, Mar. 2016.
[39] J. Wang *et al.*, "Beam codebook based beamforming protocol for multi-Gbps millimeter-wave WPAN systems," *IEEE J. Sel. Areas Commun.*, vol. 27, no. 8, pp. 1390–1399, Oct. 2009.
[40] A. Alkhateeb, O. El Ayach, G. Leus, and R. W. Heath, Jr., "Channel estimation and hybrid precoding for millimeter wave cellular systems," *IEEE J. Sel. Topics Signal Process.*, vol. 8, no. 5, pp. 831–846, Oct. 2014.
[41] J. N. Laneman, D. N. C. Tse, and G. W. Wornell, "Cooperative diversity in wireless networks: Efficient protocols and outage behavior," *IEEE Trans. Inf. Theory*, vol. 50, no. 12, pp. 3062–3080, Dec. 2004.
[42] A. Shahmansoori, G. E. Garcia, G. Destino, G. Seco-Granados, and H. Wymeersch, "5G position and orientation estimation through millimeter wave MIMO," in *Proc. IEEE Globecom Workshops*, Dec. 2015, pp. 1–6.

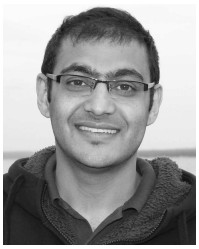

KHAGENDRA BELBASE (S'17) received the B.Eng. degree in electronics and communications engineering from the Institute of Engineering, Pulchowk Campus, Nepal, in 2010, and the M.Eng. degree from the Antenna and Radio Propagation Laboratory, Department of International Development Engineering, Tokyo Institute of Technology, Tokyo, Japan, in 2014. He is currently pursuing the Ph.D. degree with the Department of Electrical and Computer Engineering, University of Alberta, Edmonton, AB, Canada. His research interests include wireless communications theory, millimeter wave communications, wireless relaying, and stochastic geometry analysis of wireless networks.

ZHANG ZHANG received the B.Eng. and Ph.D. degrees from the Beijing University of Posts and Telecommunications, Beijing, China, in 2007 and 2012, respectively. From 2009 to 2012, he served as a Research Assistant for the Wireless and Mobile Communications Technology R&D Center, Tsinghua University, Beijing, China. He is currently with the Department of Radio Access Network Research, Huawei Technologies Co., Ltd., Shanghai, China. His current research interests include information theory and radio access technologies.

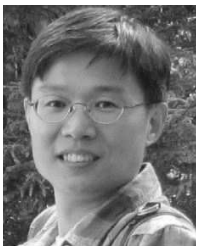

HAI JIANG (SM'15) received the B.Sc. and M.Sc. degrees in electronics engineering from Peking University, Beijing, China, in 1995 and 1998, respectively, and the Ph.D. degree in electrical engineering from the University of Waterloo, Waterloo, ON, Canada, in 2006. Since 2007, he has been a Faculty Member with the University of Alberta, Edmonton, AB, Canada, where he is currently a Professor with the Department of Electrical and Computer Engineering. His research interests include radio resource management, cognitive radio networking, and cooperative communications.

CHINTHA TELLAMBURA (F'11) received the B.Sc. degree (Hons.) from the University of Moratuwa, Sri Lanka, the M.Sc. degree in electronics from King's College, University of London, U.K., and the Ph.D. degree in electrical engineering from the University of Victoria, Canada.

He was with Monash University, Australia, from 1997 to 2002. He is currently a Professor with the Department of Electrical and Computer Engineering, University of Alberta. His current research interests include the design, modeling and analysis of cognitive radio, heterogeneous cellular networks, and 5G wireless networks.

He has authored or co-authored over 500 journal and conference papers with total citations over 14 000 and an H-index of 64 (Google Scholar). In 2017, he was elected as a fellow of the Canadian Academy of Engineering. He has received the Best Paper Awards in the Communication Theory Symposium in the 2012 IEEE International Conference on Communications (ICC), Canada, and the 2017 ICC, France. He was a recipient of the prestigious McCalla Professorship and the Killam Annual Professorship from the University of Alberta. He served as an Editor for the IEEE TRANSACTIONS ON COMMUNICATIONS from 1999 to 2011 and the IEEE TRANSACTIONS ON WIRELESS COMMUNICATIONS from 2001 to 2007 and he was an Area Editor for *Wireless Communications Systems and Theory* from 2007 to 2012.